Avrupa Bilim ve Teknoloji Dergisi
Özel Sayı 44, S. 59-64, Aralık 2022

Araştırma Makalesi

www.ejosat.com ISSN:2148-2683

European Journal of Science and Technology
Special Issue 44, pp. 59-64, December 2022

Research Article

Sensor Fusion Based on Mathematical Model of LEO Satellite

Seda (Karadeniz) Kartal[1*], Tayfun Dar[2]

[1*,2] TÜRKSAT Ar-Ge ve Uydu Tasarım Direktörlüğü, Ankara, Turkey, (ORCID: 0000-0003-4756-5490), skartal@turksat.com.tr, tdar@turksat.com.tr

(6th International Symposium on Innovative Approaches in Smart Technologies (ISAS) 2022 – 8-10 December 2022)

(**DOI:** 10.31590/ejosat.1216679)

ATIF/REFERENCE: Karadeniz Kartal, S. & Dar, T. (2022). Sensor Fusion Based on Mathematical Model of LEO Satellite *European Journal of Science and Technology*, (44), 59-64.

Abstract

In this study, the mathematical model of attitude motion is obtained for low orbit satellite (LEO) with its kinematic and dynamic equations. The mathematical model of orbit motion for LEO satellite is obtained using Kepler parameters. Sensor data are generated adding zero mean Gaussian noise to data comes from model response. These measurement data are fused using INS/GPS integration structure. Extended Kalman filter algorithm is used to sensor fusion. Compare the estimated data comes from extended Kalman filter and the actual data generated from mathematical model. It has been observed from the results that the estimated data is closest to the actual attitude data. All study is performed at the MATLAB/Simulink environment.

Keywords: LEO satellite, mathematical model, orbit model of satellite, attitude model of satellite, sensor fusion, integration navigation system

Alçak Yörünge Uydu Matematiksel Model Tabanlı Sensör Füzyonu

Öz

Bu çalışmada bir alçak yörünge uydusunun kinematik ve dinamik denklemleri elde edilerek döngüsel hareket için matematiksel model oluşturulmuştur. Kepler parametreleri kullanılarak bu alçak yörünge uydusunun yörünge hareket modeli elde edilmiştir. Döngüsel hareket modelden elde edilen yönelim bilgilerine gürültü eklenerek yönelim sensör verileri üretilmiştir. INS/GPS entegre navigasyon yapısı için sistem ve ölçüm modelleri elde edilerek farklı sensörlerden alınan yönelim bilgileri birleştirilmiştir. Sensör veri birleştirmede genişletilmiş Kalman filtre algoritmaları kullanılmıştır. Kestirilen yönelim bilgisi ile ölçülen ve gerçek yönelim bilgisi karşılaştırılmıştır. Sonuçlardan kestirilen yönelim bilgisinin gerçek yönelim bilgisine en yakın değer olduğu gözlemlenmiştir. Tüm çalışma MATLAB/Simulink ortamında gerçekleştirilmiştir.

Anahtar Kelimeler: Alçak yörünge uydu, matematiksel modelleme, yörünge modeli, döngüsel hareket modeli, sensor veri birleştirme, entegre navigasyon sistemi

* Corresponding Author: sedakaradeniz@gmail.com, skartal@turksat.com.tr

1. Introduction

Satellites are used for observation, positioning, and communication purposes as LEO (low Earth orbit), MEO (middle Earth orbit), GEO (Geosynchronous Equatorial Orbit) according to the orbit level [1], [2]. Although MEO satellites signals are commonly used for navigation system, in the recent years, low orbit satellites group's signals are used for positioning system [3], [4]. It is important that the satellites used for all this purpose should remain stable in a certain orbit and attitude for position accuracy. The orbit and attitude stability of satellite is distributed due to perturbation torques. The reaction wheels integrated the satellites generate torque to balance these perturbation torque acting on the satellite. These reaction wheels should be controlled depending on the difference between the data comes from measurement sensors on the satellite and the desired orbit and attitude information value.

For more accurate control of them, measurement data defined the satellite's orbit and attitude should be taken correctly. For this purpose, it is necessary to measure the same data from more than one sensor and these sensor data should be fused. There are many algorithms used to sensor fusion. The most used algorithm is Kalman filter [5]. Fuzzy algorithm for tunning the extended Kalman filter estimation was used to multi sensor fusion [6]. Federated Unscented Kalman filter designed for multiple satellites formation flying in LEO [7]. Sensor fusion was performed by creating an integrated navigation system [8]. INS/GPS integrated navigation structure was designed by using the position, speed and attitude error propagation equations of INS integrated into satellite body [9].

Sensor data can be generated by obtaining the mathematical model of satellite in order to analyze the sensor fusion algorithm. Obtain the orbit and attitude motion model of satellite is important for the error model due to these motion on the positioning system used the satellite's signals [10], [11].

In this study, the mathematical model for attitude and orbit motion of satellite is obtained. The angular velocity propagation of satellite is obtained with the attitude motion model. The sensor data is generated using the mathematical model response. Measured information from multiple sensors are fused with the integrated navigation system.

The remainder of this paper is organized as follows. Section 2 presents the mathematical model of attitude motion for low orbit satellite. We provide a detailed information of orbit model for low orbit satellite in Section 3. Section 4 presents integrated navigation system and sensor fusion and simulation results. Lastly, the conclusion and future work are presented in Section 5.

2. Mathematical Model of Attitude Motion for Low-Orbit Satellite

The dynamic and kinematic equations are implemented to obtain the mathematical model of low orbit satellite.

2.1 Dynamic Model

The dynamic model given the derivation of angular velocity for satellite is as [12]:

$$\dot{w}_{ib}^{b} = I_s^{-1}\left[M_D - \dot{H}_{RW}^{b} - \Omega\left(w_{ib}^{b}\right)I_s w_{ib}^{b} - \Omega(w_{ib}^{b})H_{RW}^{b}\right] \quad (1)$$

where

I_s; inertia tensor matrix of satellite

M_D; the torque based on perturbations

H_{RW}^{b}; the momentum generated by reaction wheels

$\dot{H}_{RW}^{b}$; the torque produced by reaction wheels

w_{ib}^{b}; the angular velocity of satellite in body-frame

$\Omega\left(w_{ib}^{b}\right)$; the skew-symmetric matrix based on angular velocity of satellite

The perturbation torques due to the gravity gradient, solar radiation, aerodynamic, magnetic dipole moment are affected to the attitude motion of satellite [12], [13]. This perturbation torques are balanced with reaction wheels or magnetic torque sticks. In this study, the torques generated by reaction wheels is considered the control torque $\dot{H}_{RW}^{b} = M_C$.

The inertia tensor matrix is considered diagonal matrix since the contribution of the off-diagonal matrix is small [14].

$$I_s = \begin{bmatrix} I_{sxx} & 0 & 0 \\ 0 & I_{syy} & 0 \\ 0 & 0 & I_{szz} \end{bmatrix} \quad (2)$$

The skew-symmetric matrix based on angular velocity of satellite in the x, y and z axis is as [14]:

$$\Omega\left(w_{ib}^{b}\right) = \begin{bmatrix} 0 & -w_{ib,z}^{b} & w_{ib,y}^{b} \\ w_{ib,z}^{b} & 0 & -w_{ib,x}^{b} \\ -w_{ib,y}^{b} & w_{ib,x}^{b} & 0 \end{bmatrix} \quad (3)$$

The block diagram of dynamic model of low orbit satellite obtained in Simulink environment is shown as Figure 1. As seen Figure 1, the angular velocity propagation of satellite is obtained using the inertia tensor data of satellite, reaction wheel's momentum data and torques generated by reaction wheel against the perturbation torques. So, the output of this block is the angular velocity changing in the body frame. The angular velocity in the body-frame is obtained by integrating the output of this block related to equation 1.

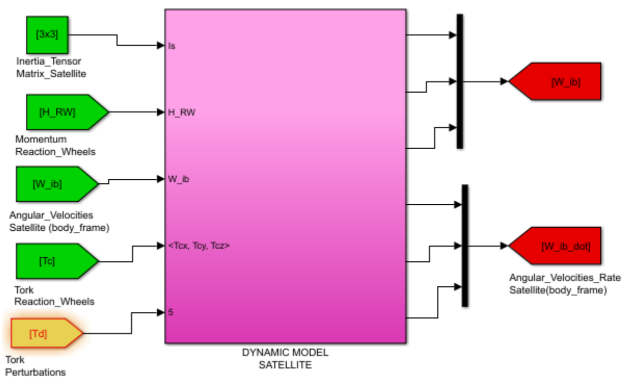

Figure 1. The Simulink block diagram of dynamic model for LEO satellite

2.1.1 Reaction Wheel Model

The reaction wheels integrated the satellites generate torque to balance the external impact forces acting on the satellite. The location and number of these wheels affect the torque produced. In this study, the reaction wheels configuration is considered as tetrahedron. The angular momentum (H_{Rw}) and generated tork of each wheel (M_C) are as [12]:

$$H_{RW} = I_{Rw} W_{Rw} \tag{4}$$

$$M_C = I_{Rw} \dot{W}_{Rw} \tag{5}$$

Each reaction wheel is considered as identical and the inertial tensor matrix parameter of each wheel is equal $I_{RW} = I_{RW,x} = I_{RW,y} = I_{RW,z}$. The location matrix of reaction wheels is given by [15]:

$$L = \begin{bmatrix} \sqrt{3}/_3 & -\sqrt{3}/_3 & -\sqrt{3}/_3 & \sqrt{3}/_3 \\ \sqrt{3}/_3 & -\sqrt{3}/_3 & \sqrt{3}/_3 & -\sqrt{3}/_3 \\ \sqrt{3}/_3 & \sqrt{3}/_3 & -\sqrt{3}/_3 & -\sqrt{3}/_3 \end{bmatrix} \tag{6}$$

The generated torque by each wheel in the x, y and z axis is written as [15]:

$$\begin{bmatrix} M_{c,x} \\ M_{c,y} \\ M_{c,z} \end{bmatrix} = L \begin{bmatrix} T_1 \\ T_2 \\ T_3 \\ T_4 \end{bmatrix} \tag{7}$$

where T_1, T_2, T_3, T_4 applied torque to each reaction wheel respectively. The derivative of angular velocity is obtained as $\dot{W}_{Rw} = \frac{M_C}{I_{Rw}}$. The tork produced by each reaction wheel at each axis is defined by:

$$T_C = \begin{bmatrix} \dot{H}^b_{RW,x} + H^b_{RW,z} W^b_{ib,z} - H^b_{RW,y} W^b_{ib,z} \\ \dot{H}^b_{RW,y} + H^b_{RW,x} W^b_{ib,z} - H^b_{RW,z} W^b_{ib,x} \\ \dot{H}^b_{RW,z} + H^b_{RW,y} W^b_{ib,x} - H^b_{RW,x} W^b_{ib,y} \end{bmatrix} \tag{8}$$

The generated torque block diagram by four reaction wheels is shown as Figure 2. As seen block diagram, the torque and momentum generated by reaction wheels using the angular velocity of satellite and the applied force to each wheel. The max torque applied to each wheel is 0.018 Nm.

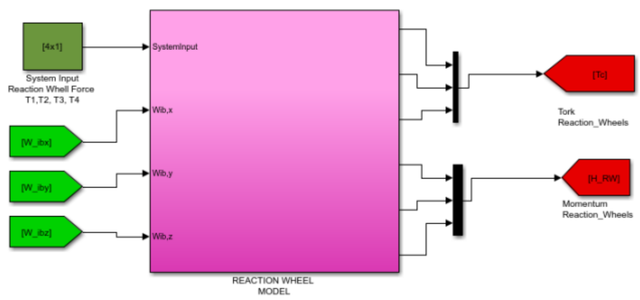

Figure 2. The Simulink block diagram for torque and momentum generated by reaction wheels

2.2 Kinematic Model

Kinematic model supply transformation between different frames. The angular velocity of satellite is transformed from body to orbit frame using the kinematic model. The transformation matrix consists of Euler angles is used to this transformation. The transformation matrix $C(q)^b_o$ defined by quaternion vectors, $[q_1 \quad q_2 \quad q_3 \quad q_4]$, are used in this study because Euler angles are undefined at some angles (90 degree) [12]. Kinematic model;

$$\dot{q} = \frac{1}{2} \Omega \left(w^b_{ob}\right) q \tag{9}$$

where $\Omega\left(w^b_{ob}\right)$ is the skew-symetric matrix in terms of angular velocity of satellite in the orbit frame and it is obtained as [12]:

$$\begin{bmatrix} w_x \\ w_y \\ w_z \end{bmatrix}^b_{ob} = \begin{bmatrix} w_x \\ w_y \\ w_z \end{bmatrix}^b_{ib} - C^b_o \begin{bmatrix} 0 \\ -w_0 \\ 0 \end{bmatrix} \tag{10}$$

where w^b_{ob} is the angular velocity of satellite in the orbit frame, w^b_{ib} is the angular velocity of satellite in the body frame. The mean motion of satellite represented by w_0 is obtained as:

$$w_0 = \sqrt{\frac{GM_e}{R^3}} \tag{11}$$

G is the gravity constant of Earth, Me is the Earth mass, R is the distance between satellite and Earth. In this study, the value of w_0 is taken as approximately 0,0069 rad/s [13]. The transformation matrix from body to orbit frame is defined as [12].

$$C(q)^b_o = \begin{bmatrix} C(q)_{11} & C(q)_{12} & C(q)_{13} \\ C(q)_{21} & C(q)_{22} & C(q)_{23} \\ C(q)_{31} & C(q)_{32} & C(q)_{33} \end{bmatrix} \tag{12}$$

$$C(q)_{11} = q_1^2 + q_4^2 - q_2^2 - q_3^2$$
$$C(q)_{12} = 2(q_1q_2 + q_3q_4)$$
$$C(q)_{13} = 2(q_1q_3 - q_2q_4)$$

$$C(q)_{21} = 2(q_1q_2 - q_3q_4)$$
$$C(q)_{22} = q_4^2 - q_1^2 + q_2^2 - q_3^2 \qquad (13)$$
$$C(q)_{23} = 2(q_2q_3 + q_1q_4)$$

$$C(q)_{31} = 2(q_2q_3 + q_1q_4)$$
$$C(q)_{32} = 2(q_1q_3 - q_1q_4)$$
$$C(q)_{33} = q_4^2 - q_1^2 - q_2^2 + q_3^2$$

The block diagram of kinematic model of satellite occured in Simulink environment is shown as Figure 3. As seen Figure 3, quaternion elements are obtained using the input data of block with mean motion value of satellite and angular velocity data of the satellite in the body frame. So, the angular velocity of the satellite can be transformed from body frame to orbit frame.

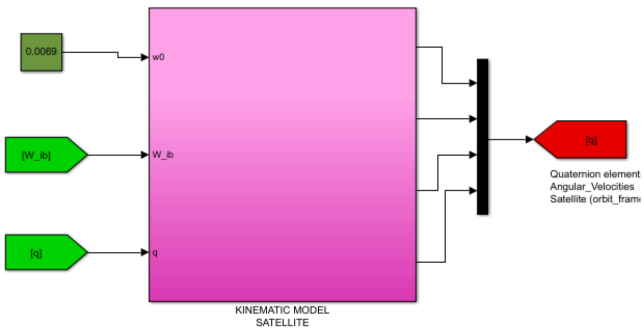

Figure 3. The Simulink block diagram of LEO kinematic model

3. Orbit Propagation Model

The orbit propagation model of LEO is obtained using Kepler parameters [9]. These parameters are orbit inclination (i), right ascension of ascending node (Ω), eccentricity (e), argument of perigee (w), mean anomaly (M), mean motion (n), eccentric anomaly (E). In this study, constant values of Kepler parameters are taken from TLE data series (Two lines element data) of FLP satellite.

The time derivation of the mean anomaly and the time derivation of eccentric anomaly are as [12], [13]:

$$M(t_0 + t) = M(t_0) + n.t \qquad (14)$$

$$E(t) = M(t) + e.sinE(t) \qquad (15)$$

$$E_{i+1} = E_i + \frac{M_i + e.\sin(E_i) - E_i}{1 - e.\cos(E_i)} \qquad (16)$$

where n, mean motion is the a

average angular velocity that defines the sizes of the ellipse. It is obtained using the Kepler's third law as:

$$n = \sqrt{\frac{\mu_e}{a^3}}, \ \mu_e = G.M_e \qquad (17)$$

where G is the gravity constant of Earth, M_e is the Earth mass. So, the position of satellite in orbit frame (r^{oc}) is obatined. The position of satellite in the Earth frame and inertial frame is obtained using the transformation matrix [12].

$$r^{OC} = a\begin{bmatrix} cosE - e \\ \sqrt{1-e^2}sinE \\ 0 \end{bmatrix} \qquad (18)$$

The perturbations torque effected to orbit motion of satellite are due to the Earth gravity harmonics, Earth tides effect, Sun and Moon gravitational effect, solar radiation pressure, atmospheric drag.

4. Integrated Navigation System and Sensor Fusion

The flow diagram of the integrated navigation and sensor fusion is shown in Figure 4. The yaw angle occured with perturbation torque and reaction wheels torque is measured by magnetometer and gyro of IMU. These sensor measurement data are fused Extended Kalman filter algorithm. System and measurement model for integrated navigation system and sensor fusion are obtained follow chapter.

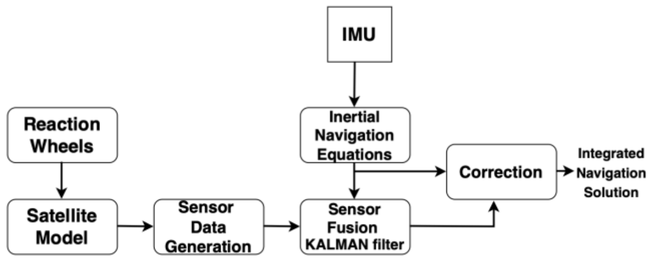

Figure 4. The flow diagram for sensor fusion and integrated navigation system

4.1 System Model

In this study, attitude error states are estimated. Extended Kalman filter algorithm is used for estimation [8]. Error states are chosen as attitude, velocity, position errors and accelerometer and gyro biases in terms of Earth frame and they are defined as [16].

$$x_{eb}^e = [\delta\varphi_{eb}^e \quad \delta v_{eb}^e \quad \delta r_{eb}^e \quad b_a \quad b_g]^T \qquad (19)$$

$\delta\varphi_{eb}^e$: attitude error vector,

δv_{eb}^e: velocity error vector,

δr_{eb}^e: position error vector.

The time derivation of attitude error as

$$\delta\dot{\varphi}_{eb}^e = \hat{C}_b^e b_g - \Omega_{ie}^e \delta\varphi_{eb}^e \qquad (20)$$

The time derivation of velocity error as

$$\dot{\delta v}^{e}_{eb} = \hat{C}^{e}_{b} b_a - (\hat{C}^{e}_{b} \hat{f}^{b}_{ib})^{\wedge} \delta\varphi^{e}_{eb} - 2\Omega^{e}_{ie} \delta v^{e}_{eb} \quad (21)$$

The time derivation of position error is given by

$$\dot{\delta r}^{e}_{eb} = \delta v^{e}_{eb} \quad (22)$$

The state-space model of system as

$$\dot{x} = Fx + Qw \quad (23)$$

where w is the system noise and taken as zero-mean Gaussian noise. F is the system matrix, Q is the system covariance matrix. System matrix is defined related to system states as:

$$F = \begin{bmatrix} -\Omega^{e}_{ie} & 0_3 & 0_3 & 0_3 & \hat{C}^{e}_{b} \\ [-\hat{C}^{e}_{b} \hat{f}^{b}_{ib} \wedge] & -2\Omega^{e}_{ie} & 0_3 & \hat{C}^{e}_{b} & 0_3 \\ 0_3 & I_3 & 0_3 & 0_3 & 0_3 \\ 0_3 & 0_3 & 0_3 & 0_3 & 0_3 \\ 0_3 & 0_3 & 0_3 & 0_3 & 0_3 \\ 0_3 & 0_3 & 0_3 & 0_3 & 0_3 \end{bmatrix} \quad (24)$$

System covariance matrix is as [16]-[17].

$$Q = \begin{bmatrix} n^2_{rg} I_3 & 0_3 & 0_3 & 0_3 & 0_3 \\ 0_3 & n^2_{ra} I_3 & 0_3 & 0_3 & 0_3 \\ 0_3 & 0_3 & 0_3 & 0_3 & 0_3 \\ 0_3 & 0_3 & 0_3 & 0_3 & 0_3 \\ 0_3 & 0_3 & 0_3 & n^2_{bad} I_3 & 0_3 \\ 0_3 & 0_3 & 0_3 & 0_3 & n^2_{bgd} I_3 \end{bmatrix} \quad (25)$$

where $n^2_{rg}, n^2_{ra}, n^2_{bad}, n^2_{bgd}$ are gyro and accelerometer noise power density, accelerometer bias power density and gyro bias power density respectively. Where σ_{ra}, σ_{rg} are standard deviation accelerometer force measurement and gyro angular velocity measurement respectively. Where τ_i is the integral time interval, σ_{bad} is the bias accelerometer and σ_{bgd} is the bis of gyro [16]-[17].

$$n^2_{ra} = \sigma^2_{ra} \tau_i \quad (26)$$

$$n^2_{rg} = \sigma^2_{rg} \tau_j \quad (27)$$

$$n^2_{bad} = \sigma^2_{bad} \tau_{bad} \quad (28)$$

$$n^2_{bgd} = \sigma^2_{bgd} \tau_{bgd} \quad (29)$$

Since the inertial sensor data used to navigation system is the discrete time, system model and measurement model should be discrete [16].

$$x_{k+1} = \emptyset_k x_k + w_k \quad (30)$$

where $\emptyset_k$ is the system transient matrix and F is the system state matrix. It is assumed that the F matrix is constant at the time interval $\Delta t_{k+1} - t_k$. So, the system transient matrix is defined as [16].

$$\emptyset_k = e^{F\Delta t} = I + F + \frac{(F\Delta t)^2}{2!} \quad (31)$$

4.2 Measurement Model

Measurement model consists the attitude errors. Yaw angle is obtained by integrating angular velocity comes from gyro of IMU. Yaw angle is measured also by magnetometer. These different sensor data are fused in the ECEF. The measurement error variation vector for extended Kalman filter as [16].

$$\delta z_k = \tilde{\varphi}_{mc} - \tilde{\varphi}_o \quad (32)$$

The measurement matrix, H_k, is obtained as:

$$H_k = \begin{bmatrix} 1\,0\,0\,0\,0\,0\,0\,0\,0\,0\,0\,0\,0\,0\,0 \\ 0\,1\,0\,0\,0\,0\,0\,0\,0\,0\,0\,0\,0\,0\,0 \end{bmatrix} \quad (33)$$

Measurement covariance matrix is chosen as follow R_k. R11 and R22 are related to measurement sensitivity of gyroscope and magnetic compass respectively.

$$R_k = \begin{bmatrix} R11 & 0 \\ 0 & R22 \end{bmatrix} \quad (34)$$

4.3 Simulation Results

In this study, different force is applied to each reaction wheel. Perturbations torques (considered due to gravity gradient) also effected to satellite motion. Since the reaction wheels are not controlled in this study, the satellite motion is not stable. So, the satellite rotates in the x, y and z axis with roll, pitch, and yaw angles. Perturbations torques applied to satellite motion in the x, y and z axis are shown in Figure 5.

The yaw angle from the attitude mathematical model of satellite is considered as the real yaw angle data. The measurement data comes from gyro and magnetometer are generated by adding Gaussian noise to actual data comes from the mathematical model of satellite. It is assumed that the accuracy of magnetometer is higher than the gyro. The yaw angles measured by these different sensors are fused using the integrated navigation system designed by Kalman filter algorithm. Figure 6 shows the measured yaw angle comes from gyro and magnetometer, actual yaw angle comes from mathematical model and estimated yaw angle comes from Kalman filter output. As seen Figure 6, the estimated yaw angle is closest to actual yaw angle.

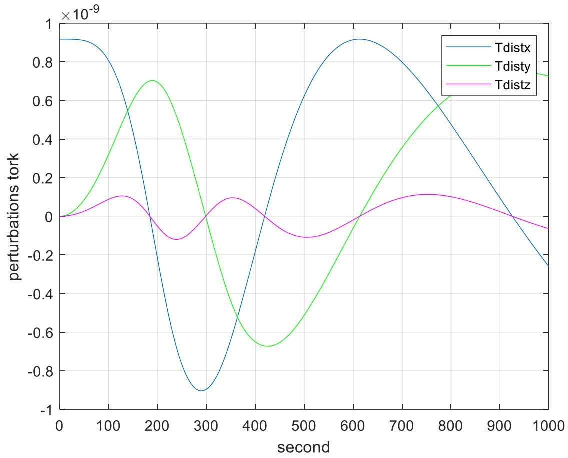

Figure 5. Perturbations torques applied to satellite in the x, y and z axis

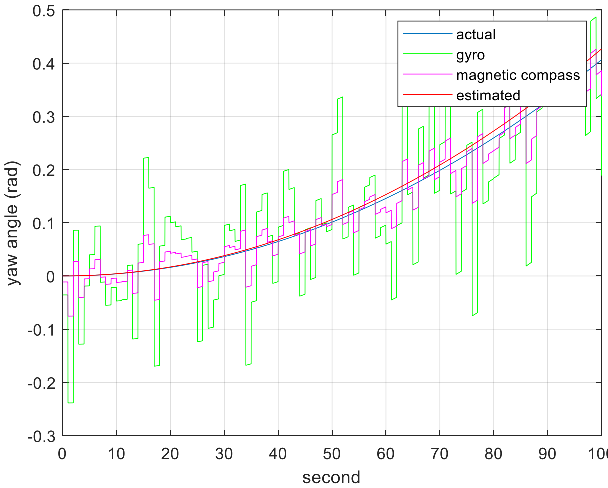

Figure 6. Actual yaw angle (blue line), measurement yaw angle from gyro (green line), measurement yaw angle from magnetometer (pink line), estimated yaw angle comes from Kalman filter (red line)

5. Conclusion

In this study, the attitude mathematical model of low orbit satellite is obtained with dynamic and kinematic equations of motion. The measurement data comes from magnetometer and gyro are generated using the attitude mathematical model response. System model and measurement model are occured for INS/GPS integrated navigation system. Different sensor data are fused with extended Kalman filter algorithm. All this study is performed in MATLAB/Simulink environment. Orbit propagation model of satellite is obtained using Kepler parameters but the sensor data generated with orbit motion model response is not used in this study. Perturbations torques will be improved and implemented to GEO satellite and the different controllers of reaction wheel will be designed for the future work.

References

[1] F. Vatalaro, G.E. Corazza, C. Ferralli, "Analysis of LEO, MEO and GEO global mobile satellite systems in the presence of interference and fading", IEEE Journal on Selected areas in Communication.

[2] C. Saunders, "The role of small satellites in military communications", IET Seminar on Military Satellite Communication, 2013.

[3] Prol F. S., Ferre R. M., Saleem Z., "Position, Navigation, and Timing (PNT) Through Low Earth Orbit (LEO) Satellites, IEEE Access, 2022.

[4] Neinovare M., Khalife J. and Kassas Z. M., "Exploting starlink Signals for Navigation: First Results", GNSS Conferences, 20-24 September, 2021.

[5] B. Gao, G. Hu, Y. Zhong, and X. Zhu, "Cubature Kalman Filter with Both Adaptability and Robustness for Tightly-coupled GNSS/INS Integration," IEEE Sensors Journal, 2021.

[6] Tan N. D., Vinh T. Q., Tuyen B. T., "A new approach for Small Satellite Gyroscope and Star Tracker Fusion", Indian Journal of Science and Technologgy, Vol 9(17), 2016

[7] Ilyas M., Lim J., Lee J. G., Park C. G., "Federated unscented Kalman filter design for multiple satellites formation flying in LEO", IEEE 2008 International conference on control automation and systems

[8] I. Lee, H. Li, N. Hoang, and J. Lee, "Navigation system development of the underwater vehicles using the GPS/INS sensor fusion," 14th International Conference on Control, Automation and Systems, pp. 610– 612, 2014.

[9] R. Song, and Y. Fang, "Vehicle state estimation for INS/GPS aided by sensors fusion and SCKF-based algorithm," Mechanical Systems and Signal Processing, vol. 150, pp. 107315, 2021.

[10] Sadaf Tafazoli, Mohammad Reza Mosavi, "Performance Improvement of GPS GDOP Approximation Using Recurrent Wavelet Neural Network", Journal of Geographic Information System, 2011, 3, 318-322

[11] Tahsin M., Reza T., Sultan S., Haider M. "Analysis of DOP and its Preciseness in GNSS Position Estimation "Int'l Conf. on Electrical Engineering and Information & Communication Technology (ICEEICT) 2015

[12] Kutlu Aykut "Design of Kalman Filter Based Attitude Determination Algorithms for a LEO Satellite and for a Satellite Attitude Control Test Setup", METU, Master Thesis.

[13] Karataş Soner, "LEO SATELLITES: Dynamic Modelling, Sımulatıons and Some Nonlinear Attitude Control Techniques", METU, Master Thesis.

[14] Efendioğlu Gamze, "Design of Kalman Filter based Attitute Determination and Control Algorithms for a LEO Satellite", METU, Master Thesis.

[15] Kök İbrahim, "Comparison and Analysis of Attitude Control Systems of a Satellite Using Reaction Wheel Actuators" Lulea University of Technology, METU, Master Thesis.

[16] Groves P. "Principles of GNSS, Inertial, and Multisensor Integrated Navigation Systems"

[17] Karadeniz Kartal S., Leblebicioğlu M. K., Ege E., "Acoustic-based navigation and system identification of an unmanned underwater vehicle", Transaction Measurement and Control, 2019